Available online at www.sciencedirect.com
ScienceDirect
Dynamics of Atmospheres and Oceans
xxx (2008) xxx–xxx
dynamics of atmospheres and oceans
www.elsevier.com/locate/dynatmoce

Global monsoon: Dominant mode of annual variation in the tropics

Bin Wang *,[1], Qinghua Ding

Q1 *Department of Meteorology and International Pacific Research Center, School of Ocean and Earth Science and Technology, University of Hawaii, 2525 Correa Road, Honolulu, HI 96822, USA*

Received 1 October 2006; received in revised form 6 May 2007; accepted 7 May 2007

Abstract

This paper discusses the concept of global monsoon. We demonstrate that the primary climatological features of the tropical precipitation and low-level circulation can be represented by a three-parameter metrics: the annual mean and two major modes of annual variation, namely, a solstitial mode and an equinoctial asymmetric mode. Together, the two major modes of annual cycle account for 84% of the annual variance and they represent the global monsoon. The global monsoon precipitation domain can be delineated by a simple monsoon precipitation index (MPI), which is the local annual range of precipitation (MJJAS minus NDJFM in the Northern Hemisphere and NDJFM minus MJJAS in the Southern Hemisphere) normalized by the annual mean precipitation. The monsoon domain can be defined by annual range exceeding 300 mm and the MPI exceeding 50%.

The three-parameter precipitation climatology metrics and global monsoon domain proposed in the present paper provides a valuable objective tool for gauging the climate models' performance on simulation and prediction of the mean climate and annual cycle. The metrics are used to evaluate the precipitation climatology in three global reanalysis products (ERA40, NCEP2, and JRA25) in terms of their pattern correlation coefficients and root mean square errors with reference to observations. The ensemble mean of the three analysis datasets is considerably superior to any of the individual reanalysis data in representing annual mean, annual cycle, and the global monsoon domain. A major common deficiency is found over the Southeast Asia-Philippine Sea and southeast North America-Caribbean Sea where the east–west land–ocean thermal contrast and meridional hemispheric thermal contrast coexist. It is speculated that the weakness is caused by models' unrealistic representation of Subtropical High and under-represented tropical storm activity, as well as by neglecting atmosphere–ocean interaction in the reanalysis. It is recommended that ensemble mean of reanalysis datasets be used for improving global precipitation climatology and water cycle

* Corresponding author. Tel.: +1 808 956 2563; fax: +1 808 956 9425.
E-mail address: wangbin@hawaii.edu (B. Wang).
[1] A visiting professor at the Marine Environmental College, Ocean University of China, Qingdao, China.

0377-0265/$ – see front matter © 2008 Published by Elsevier B.V.
doi:10.1016/j.dynatmoce.2007.05.002

Please cite this article in press as: Wang, B., Ding, Q., Global monsoon: Dominant mode of annual variation in the tropics, Dyn. Atmos. Oceans (2008), doi:10.1016/j.dynatmoce.2007.05.002

budget. This paper also explains why the latitudinal asymmetry in the tropical circulation decreases with altitude.

Keywords: Global monsoon; Precipitation metrics; Domain; Monsoon precipitation index; Annual variation; Tropical general circulation

1. Introduction

Following the annual variation of the solar zenith angle, a reversal of the temperature gradient between the Northern and Southern Hemispheres and between the land and the adjacent oceans gives rise to the annual variation of the global general circulation. Both the annual mean and the annual cycle vary on longer time scales, from multi-decadal to orbital and tectonic time scales. But, for convenience, here we assume that the magnitude of the changes in "climatology" are negligibly small compared to relatively large year-to-year climate fluctuations, thus, we treat climatology as the "invariant" part of climate, for which the departures from this climatology are referred to as climate variation ("anomalies"). Such climatology is often practically determined by compiling a 30-year mean annual cycle of the atmosphere (Guttman, 1989).

While the tropical general circulation has been previously described in detail (e.g., Hastenrath, 1991; Trenberth et al., 2000), a comprehensive description of tropical precipitation climatology has only become possible recently owing to the accumulation of satellite measurements of oceanic precipitation, which now span from 1979 to the present. While the satellite-based precipitation data may have considerable uncertainties in their magnitude, the data provide reliable spatial–temporal variations and extremely valuable global coverage.

Emphasis is placed on analysis of precipitation, because precipitation plays an essential role in determining Earth's general circulation and hydrological cycle and it holds a key in linking external radiative forcing and the atmospheric circulation. About 56% of the total precipitation on Earth falls in the tropics between the Tropic of Cancer (23.5°N) and the Tropic of Capricorn (23.5°S), based on the Climate Prediction Center's Merged Analysis of Precipitation (CMAP) (Xie and Arkin, 1997). The latent heat released in precipitation plays a dominant role in driving tropical circulations and supplying moisture to the middle and high latitudes. The latent energy released in precipitation also plays a vital role in balancing radiative heat loses. Therefore, a global analysis of precipitation is of central importance.

Considering the physical principle of conservation of mass, moisture, and energy as it applies to the global atmosphere and its exchange of energy with the underlying surfaces, analysis of the major modes of climatology in global tropics and subtropics is more meaningful (Trenberth et al., 2000). The monsoon climate is characterized by annual reversal of prevailing surface winds (Ramage, 1971) and by a contrast between rainy summer and dry winter (Webster et al., 1998). Trenberth et al. (2000) depicted a monsoon system as global-scale persistent overturning of the atmosphere, throughout the tropics, that varies according to the time of year. In essence, the monsoon arises from and manifests itself as a response of the coupled atmosphere–land–ocean system to annual variation of the solar forcing. In the present study, we use both the annual reversal of surface winds and the contrast between wet summer and dry winter to delineate the global monsoon domain.

Major questions addressed in this paper include: (1) How does the tropical precipitation and low-level circulation respond to solar radiative heating forcing? And what are the major modes

Please cite this article in press as: Wang, B., Ding, Q., Global monsoon: Dominant mode of annual variation in the tropics, Dyn. Atmos. Oceans (2008), doi:10.1016/j.dynatmoce.2007.05.002

of their annual variations? (2) How well do the reanalyses represent these major modes of climatology? And (3) Why does the latitudinal asymmetry in the tropical circulation decreases with height? The goal of the present analysis is to further our understanding about the physical processes behind the tropical hydrological cycle and the coupled atmosphere–land–ocean system respond to the solar radiative forcing on an annual time scale. We aim to extract major modes of climatology and use them to construct metrics for assessing climate models' performances. Our method is to describe the annual cycle in terms of the major modes of multivariable empirical orthogonal function (MV-EOF) analysis. The physical interpretation of these modes can shed light on the fundamental features and the driving mechanisms of the annual cycle.

2. Observed time-mean precipitation and circulation

The datasets used to compute the climatological annual cycle in this study consist of (1) CMAP, which is produced by merging rain gauge data and five kinds of satellite estimates; (2) the National Centers for Environmental Prediction (NCEP)-Department of Energy (DOE) reanalysis 2 data (NCEP2) (Kanamitsu et al., 2002); (3) the European Centre for Medium-Range Weather Forecasts (ECMWF) 40-year Reanalysis (ERA40) (Uppala et al., 2005), which involves comprehensive use of traditional observations and satellite data, and (4) Japanese 25-year ReAnalysis (JRA25) (Onogi et al., submitted for publication). The time period to construct climatological annual cycle for each dataset is from 1979 to the latest available time.

2.1. On the longitudinal and latitudinal asymmetry in annual mean precipitation

While the latitudinal distribution of the annual mean solar radiative forcing is nearly symmetric about the equator and is invariant with longitude, the tropical precipitation and low-level circulation display remarkable longitudinal asymmetries. Fig. 1 shows annual mean precipitation, which exhibits significant longitudinal asymmetries. Between 30°S and 30°N, the Eastern Hemisphere receives 4.84×10^{14} kg day^{-1} in precipitation, which is about 1.3 times the precipitation that falls in the tropical Western Hemisphere (3.78×10^{14} kg day^{-1}). In particular, about 47% of the total tropical rains fall in the Indo-Pacific warm pool (60–180°E), which occupies only one-third of the global tropics.

The well-known latitudinal asymmetry in precipitation exists only in the Western Hemisphere deep tropics between 20°S and 20°N, where the precipitation in the northern tropics (0–20°N: 1.86×10^{14} kg day^{-1}) is 1.8 times that in the southern tropics (0–20°S), because the mean Intertropical Convergence Zone (ITCZ) is located in the Northern Hemisphere (Fig. 1a). If, however, the precipitation between 30°S and 30°N is concerned, the Southern Hemisphere (SH) and Northern Hemisphere (NH) have nearly equal amounts of precipitation in the Western Hemisphere, because a large amount of precipitation falls in the South Pacific Convergence Zone (SPCZ), in which a large portion of the precipitation is located poleward of 20°S. It is the subtropical portion of the SPCZ precipitation zone that reduces the latitudinal asymmetry in the Western Hemispheric precipitation. In the Eastern Hemisphere, the precipitation is nearly symmetric around the equator: the precipitation in the NH tropics (0–20°N) amounts 2.02×10^{14} kg day^{-1}, which is about the same as its SH counterpart (2.05×10^{14} kg day^{-1}). Overall, the global mean precipitation between 30S and 30N is nearly symmetric about the equator.

While the seasonal march of precipitation zone closely follows that of boundary layer convergence zone, for the annual mean fields, the maximum precipitation zone tends to coincide

Please cite this article in press as: Wang, B., Ding, Q., Global monsoon: Dominant mode of annual variation in the tropics, Dyn. Atmos. Oceans (2008), doi:10.1016/j.dynatmoce.2007.05.002

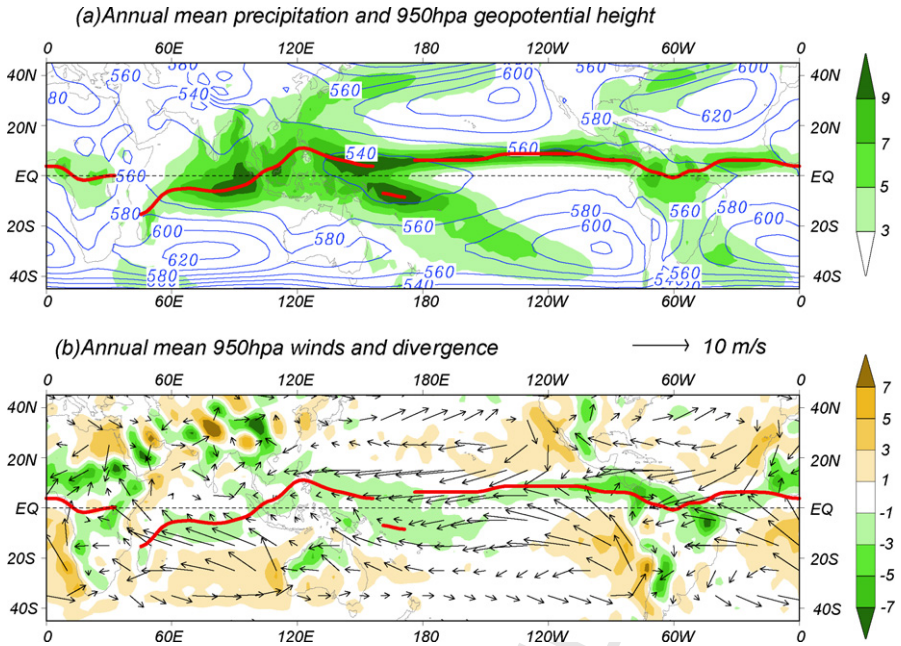

Fig. 1. (a) Annual mean precipitation (shading, unit: mm day^{-1}) and 950 hPa geopotential height (contours, unit: 10 m). (b) Annual mean winds (vectors in units of m s^{-1}) at 950 hPa and wind divergence in units of (10^{-6} s^{-1}) (shading). The red line indicates the annual mean maximum precipitation over the tropics. (For interpretation of the references to color in this figure legend, the reader is referred to the web version of the article.)

with the boundary-layer wind convergence only over the Indo-Pacific Ocean, but not over the Atlantic Ocean and Africa (Fig. 1b). Further, in the deep tropics, the surface convergence does not coincide with the minimum pressure due to the ageostrophic nature of the equatorial boundary layer motion. Wang and Li (1994) have shown that the maximum boundary layer convergence is located in the equatorward side of the minimum surface pressure where the surface winds blow poleward and eastward, because near the equator, not only the low pressure but also the poleward and eastward flows generate boundary layer convergence.

It is of interest to note that outside of the 20° latitudes, there are four major precipitation zones that all tilt eastward and poleward in association with the oceanic storm tracks in the North and South Pacific and in the North and South Atlantic. In these regions, the mean precipitation does not coincide with boundary-layer wind convergence. This is one of the fundamental differences between the tropics and the extratropics.

2.2. *Why the latitudinal asymmetry in the tropical circulations decreases with height*

The latitudinal variation of the precipitation heating has important implications in understanding the tropical general circulation. Obviously, the boundary-layer winds show considerable longitudinal and latitudinal asymmetries (Fig. 1a), which are dynamically consistent with those in precipitation. However, the latitudinal asymmetry in circulation decreases upward, and in the upper troposphere, the annual mean circulation shows a prominent, equatorial symmetric structure (Fig. 2a). Therefore, questions arise: Why does the latitudinal symmetry increase with height, and why is the upper level circulation so symmetric about the equator?

Please cite this article in press as: Wang, B., Ding, Q., Global monsoon: Dominant mode of annual variation in the tropics, Dyn. Atmos. Oceans (2008), doi:10.1016/j.dynatmoce.2007.05.002

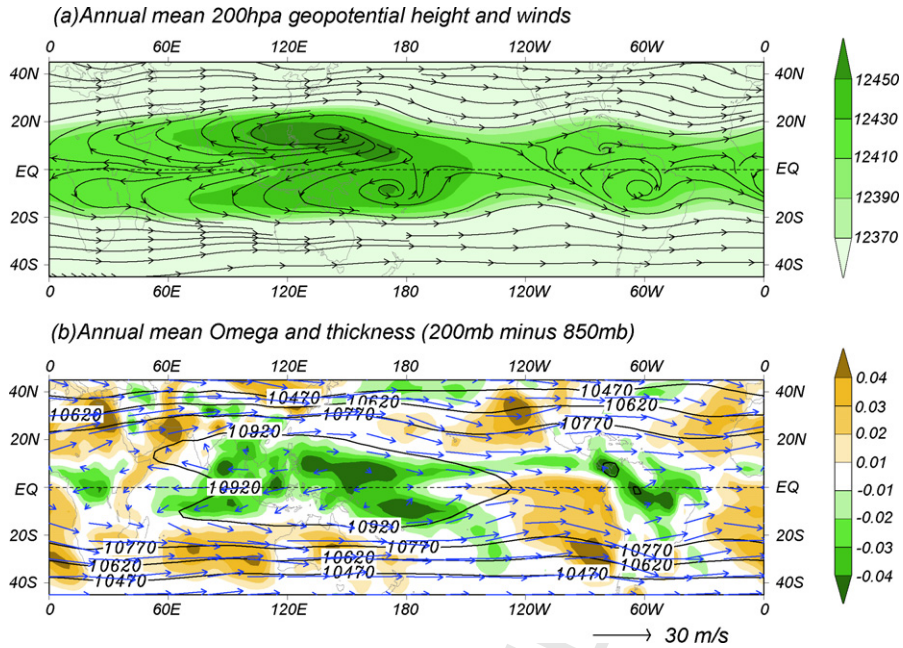

Fig. 2. (a) Annual mean geopotential heights (shading in units of 10 m) and streamline at 200 hPa. (b) Annual mean geopotential thickness (contours in units of 10 m) and thermal winds between 850 and 200 hPa (200 hPa-minus-850 hPa). Shading indicates 500 hPa vertical pressure velocities in units of Pa s^{-1}.

If the total winds and geopotential at 200 hPa are viewed as a sum of a zonal mean component and a departure from it – the eddy component – one can imagine that the tropospheric circulation is primarily baroclinic: the upper tropospheric eddy (Fig. 2a) tends to be 180° out of phase with the lower tropospheric eddy (Fig. 1a). Further, as shown in Fig. 2b, the thermal winds and the geopotential thickness between 850 and 200 hPa display notable symmetric peculiarity between the Tropics of Cancer and Capricorn. It is the equatorial symmetry in the deep-layer averaged thermal winds that gives rise to the upper tropospheric symmetric circulation shown in Fig. 2a. The reason is that the geopotential thickness and thermal winds between 200 and 850 hPa bear a close similarity to the 200 hPa circulations (Fig. 2b). Then, a new question presents itself: What determines the equatorial symmetry in the deep-layer mean thermal winds?

The deep-tropospheric thermal winds result from the latent heat released in the tropical precipitation. As shown in Fig. 2b, the upward motion in the middle of the atmosphere tends to coincide well with regions of heavy precipitation, suggesting that the diabatic heating released in precipitation is approximately balanced by the adiabatic cooling associated with the vertical motion (Charney, 1971). The symmetric patterns of the thickness and thermal winds can be understood as a Kelvin–Rossby wave response to the precipitation heating. As seen from Fig. 1a, the precipitation latent heating is maximized in the western equatorial Pacific. According to the theory of Matsuno (1966), Webster (1972), and Gill (1980), in the upper level, the eastward propagation of equatorial Kelvin waves results in the westerlies in the Western Hemisphere and the most equatorially trapped symmetric Rossby waves generate equatorial easterlies and double anticyclones residing on each side of the equator in the Eastern Hemisphere. The Rossby wave response has a much longer zonal scale (Fig. 2b) compared to what is expected from the Gill pattern excited

Please cite this article in press as: Wang, B., Ding, Q., Global monsoon: Dominant mode of annual variation in the tropics, Dyn. Atmos. Oceans (2008), doi:10.1016/j.dynatmoce.2007.05.002

by an isolated heat source. This feature in Rossby wave response is due to the elongated, twin off-equatorial tails of the latent heat source extending westward to the tropical Indian Ocean (Fig. 1a). Another factor is that the response of the upper level circulation to precipitation heating has a larger meridional scale: the Rossby radius of deformation that measures the equatorial trapping scale increases with height due to the upward increase in the stratification. Therefore, the upper level circulation reflects the impact of precipitation in a broader latitudinal extent, say from 20°S to 20°N. In the Eastern Hemisphere, the precipitation in the NH tropics (0–20°N) is about the same as its SH counterpart (Section 2a), thus the gross distribution of precipitation heating is symmetric about the equator, and the corresponding upper tropospheric circulation exhibits prominent equatorial symmetry.

The quasi-balance between the precipitation heating and diabatic cooling associated with vertical motion (Fig. 2b) implies that the tropical temperature gradients, and thus the horizontal advection of temperature, are negligibly small except in the northern edges of the equatorial cold tongue in the boundary layer. Of note is that while the imbalance between the upward motion-induced adiabatic cooling and the precipitation-induced diabatic heating is small, it is vitally important. The temperature at 500 hPa shows, on average, a positive co-variability with rising motion in the precipitating regions (Fig. 2b), implying that the generation of available potential energy in the tropics comes from thermodynamically direct circulation.

3. Observed annual variation in precipitation and low-level circulation

As mentioned in Section 1, we extract major modes of seasonal variation using multi-variable EOF (MV-EOF) analysis of the 12-month climatology. For the details of the methodology the readers are referred to Wang (1992).

3.1. The solstitial mode

Fig. 3 presents the spatial patterns of the first three MV-EOF modes of the annual cycle of precipitation and 850 hPa winds along with their corresponding principal components. The leading mode accounts for 71% of the total variance. Its spatial pattern shows a contrast between the NH and SH, although the asymmetry is not a mirror image about the equator (Fig. 3a). The differing longitudinal locations of the precipitation between the NH and SH are mainly due to the two hemispheres' differences in land distribution and topography. The 850 hPa zonal wind dominates the total wind speed over the tropics. The leading mode of the 850 hPa zonal wind also shows an equatorial antisymmetric structure in the tropic with westerlies in the NH and easterlies in the SH, resembling a boreal summer tropical monsoon circulation.

The principal component of the first MV-EOF mode shows an annual variation with a maximum in July–August and a minimum in January–February, implying an annual reversal of the flow pattern (Fig. 3d). Note that the spatial pattern of the leading mode is extremely similar to the June–September (JJAS) minus December–March (DJFM) precipitation pattern (Fig. 4a). Thus, the first mode may be called the solstitial mode, and it reflects the impact of the antisymmetric solar forcing with a 1–2-month delay in atmospheric circulation.

3.2. The equinoctial asymmetric mode

The second MV-EOF mode, which accounts for 13% of the total variance, also has an annual period but the maximum and minimum occur around April and October, respectively (Fig. 3d).

Please cite this article in press as: Wang, B., Ding, Q., Global monsoon: Dominant mode of annual variation in the tropics, Dyn. Atmos. Oceans (2008), doi:10.1016/j.dynatmoce.2007.05.002

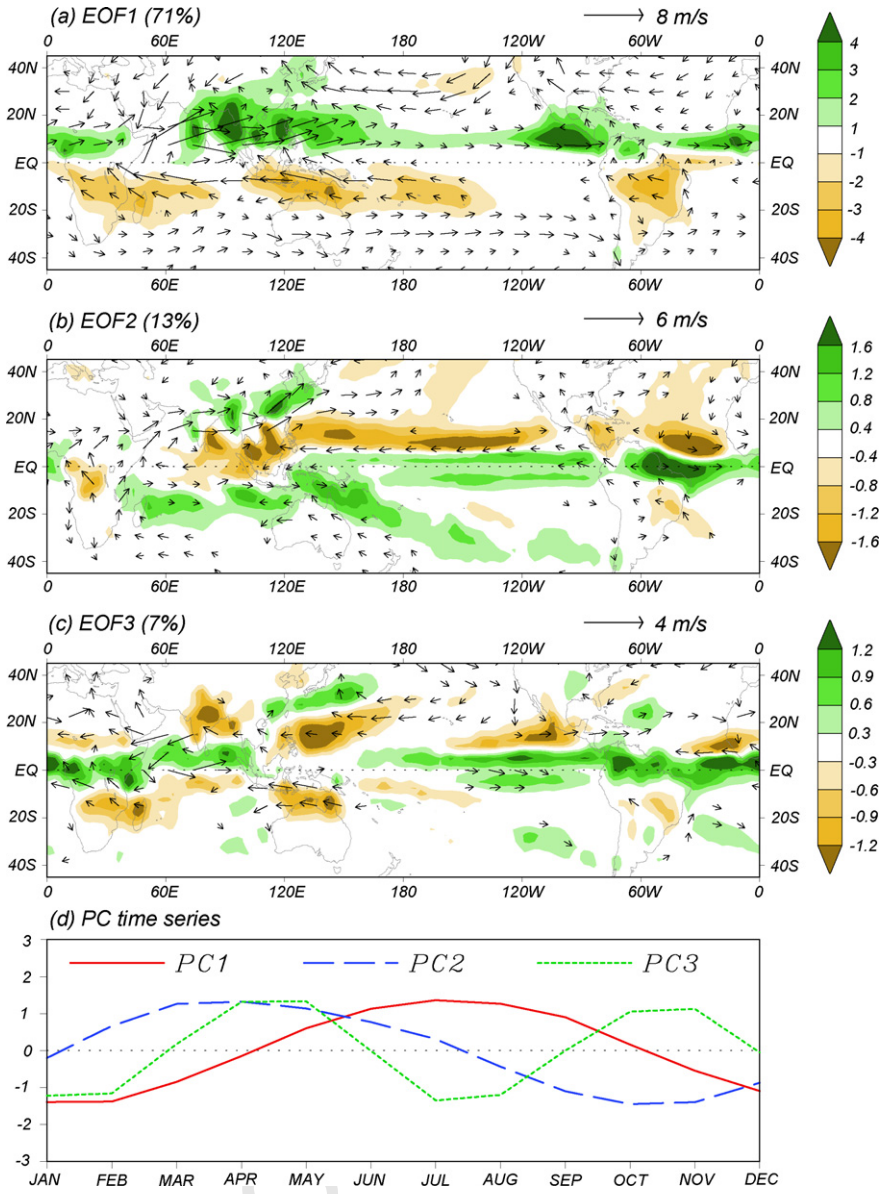

Fig. 3. (a–c) The spatial patterns of the first three multi-variable EOF modes of the climatological monthly mean precipitation (shading, unit: mm day^{-1}) and the winds (vectors in units of m s^{-1}) at 850 hPa, and (d) their corresponding normalized principal components. Winds with wind speed less than 1 m s^{-1} are omitted.

The spatial pattern of MV-EOF 2 resembles the April–May (AM) minus October–November (ON) precipitation pattern, shown in Fig. 4b. Therefore, the second EOF represents the asymmetric patterns between the two transitional seasons, or the spring-fall asymmetry, for short. The spring-fall asymmetry is one of the fundamental features of the seasonal variation in the tropical circulations, and especially the asymmetric location of the spring and fall ITCZ (Lau and Chan, 1983; Meehl, 1987), which deserves further discussion below.

Please cite this article in press as: Wang, B., Ding, Q., Global monsoon: Dominant mode of annual variation in the tropics, Dyn. Atmos. Oceans (2008), doi:10.1016/j.dynatmoce.2007.05.002

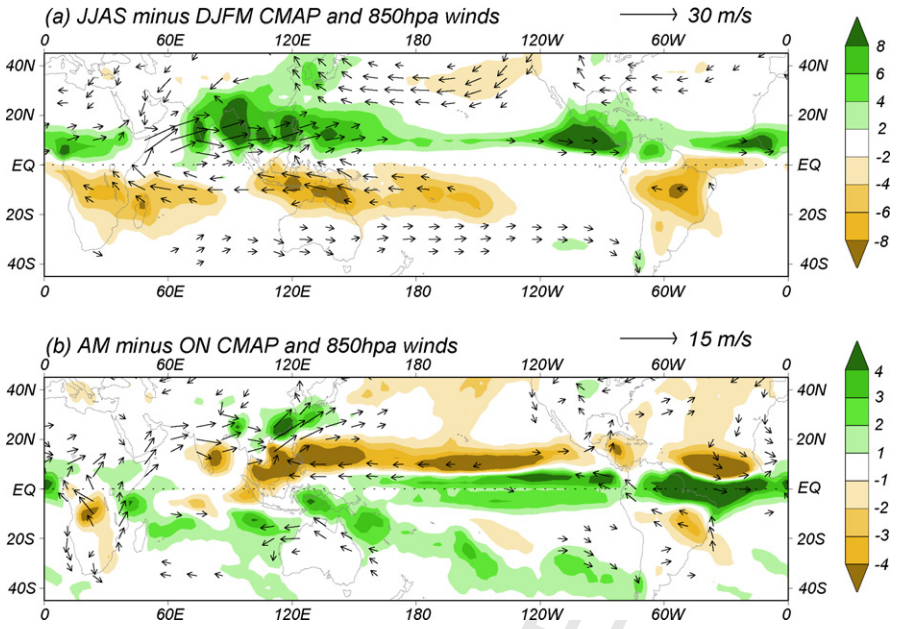

Fig. 4. (a) Solstitial mode of the annual variation as described by the differential precipitation rate (mm day^{-1}) and the 850 hPa winds between June–September and December–March (namely, JJAS minus DJFM). (b) Equinoctial asymmetric modes as described by the April–May mean minus the October–November mean precipitation rate (mm day^{-1}) and the 850 hPa winds. Winds with wind speed less than 4 and 2 m s^{-1} are omitted in (a) and (b), respectively.

How to interpret the second MV-EOF mode? In the Eastern Hemisphere, the wind departure is primarily associated with spring-fall asymmetry in the Asian–Australian monsoon precipitation. The reason is that in northern spring, the Eurasian continent warms up rapidly due to its small thermal inertia compared to the adjacent oceans. The warming sets up a continental low-pressure area and reinforces the westerlies along the southern edge of the continent. Thus, in April and May, heavy precipitation occurs along the coast of Southeast Asia, from the Bay of Bengal through southern China to Okinawa, Japan. This enhanced rain belt reflects the establishment of the planetary-scale Asian summer monsoon rain during May (e.g., Wang and Lin, 2002). In contrast, during northern fall, the rapid cooling of the Eurasian continent induces a high-pressure perturbation over the continent, and the northeasterly winter monsoon starts in October and November over the South Asian marginal seas. As a result, strong precipitation remains over the Philippine Sea due to the large ocean thermal inertia, which delays the retreat of the rainy season and prolongs tropical cyclone activity in the region. The enhanced rainfall over the southern South China Sea, Malaysia and Sri Lanka is associated with the establishment of the northern winter monsoon which enhances the precipitation on the upslope of the mountains and coastal topography. Chang et al. (2005) have discussed this spring-fall asymmetry in great detail. They attributed the spring-fall asymmetry to a combination of asymmetric wind-terrain interaction and low-level divergence asymmetry, which are both induced by different land–ocean thermal inertia over Asian–Australian monsoon region. Additionally, it seems likely that many other factors – such as the SST gradient between the warm pool and the eastern equatorial Pacific's cold tongue, cold surge and internal atmospheric dynamics – would play a role in maintaining this spring-fall asymmetry.

Please cite this article in press as: Wang, B., Ding, Q., Global monsoon: Dominant mode of annual variation in the tropics, Dyn. Atmos. Oceans (2008), doi:10.1016/j.dynatmoce.2007.05.002

In the Western Hemisphere, the spring-fall asymmetry is associated with seasonal variations in the equatorial SST cold tongues in the Pacific and Atlantic Oceans, which are warmest in March and April, thereby drawing ITCZ toward the equator, and coldest in September and October, which then suppresses equatorial convection and enhances the off-equatorial ITCZ. The April–May precipitation peak and the October–November precipitation valley are consistent with the seasonal variation of the equatorial SST cold tongue with approximately a 1-month delay. Equatorial South America is located in between the two cold tongues, and thus, the seasonal variation in precipitation follows the variation over the adjacent cold tongue regions, exhibiting similar spring-fall asymmetry.

The peculiar annual cycle in cold tongue regions is due to the influence of the ocean processes (rather than surface heat flux) that is driven by atmosphere–ocean interaction. From a meteorological point of view, the remarkable asymmetries in rainfall have been largely attributed to the asymmetries in the sea surface temperature (SST) distribution (Fig. 1). However, from oceanographic point of view, the SST distribution itself is largely determined by atmospheric winds. The easterly trades-induced upwelling forms the equatorial cold tongues in the eastern Pacific and Atlantic. The peculiar annual variation of the equatorial cold tongue is a result of the response of the coupled atmosphere–ocean–land system to the solar forcing (Wang, 1994). The air–sea interaction and the northwest–southeast oriented coastline of the North and South America play essential roles in displacing the ITCZ to the Northern Hemisphere (e.g., Philander et al., 1996) and in maintaining an annual cycle of SST that is more consistent with the Southern Hemisphere (Mitchell and Wallace, 1992). As such, both the distribution of SST and the distribution of precipitation are also determined by the response of the coupled atmosphere–ocean–land to external solar forcing.

3.3. The semi-annual mode

The third MV-EOF, which accounts for only 7% of the total variance, is characterized by a semi-annual cycle with highs in May and November and lows in February and August (Fig. 3d). What factors contribute to the third mode?

Near the equator, this is essentially an equinoctial symmetric mode, in which the atmospheric response lags behind the semi-annual component of the solar forcing by 1–2 months. The spatial pattern of the equinox mode shows enhanced rainfall near the equator and suppressed rainfall in the off-equatorial monsoon region. The enhanced equatorial rainfall follows the maximum solar forcing due to the sun crossing the equator twice a year.

In the off-equatorial monsoon regions, however, this semi-annual variation is an artifact of the asymmetric seasonal distribution of precipitation between the wet and dry seasons (Wang, 1994). In the monsoon region, wet summer is often shorter but with a concentrated rainy period in comparison of a "flat" and dry winter. This seasonal asymmetric distribution of monsoonal rainfall gives rise to a complementary semi-annual component.

In summary, the major modes of climatology in tropical precipitation and low-level circulation may be described by the annual mean, the solstitial mode, and the spring-fall asymmetric mode. The first two major modes of seasonal variations reflect the global monsoon, by and large. The transitional seasons are shorter than the solstice seasons. For this reason, the four seasons of precipitation may be better delineated by AM (April and May), JJAS (June to September), ON (October and November), and DJFM (December to March). This delineation of the season contrasts the traditional view that divides a calendar year into four even seasons: March, April, and May (MAM); June, July, and August (JJA); September, October, and November (SON); and December, January, and February (DJF).

Please cite this article in press as: Wang, B., Ding, Q., Global monsoon: Dominant mode of annual variation in the tropics, Dyn. Atmos. Oceans (2008), doi:10.1016/j.dynatmoce.2007.05.002

4. Defining the global monsoon domain

The global monsoon arises from and manifests itself as a response of the coupled atmosphere–land–ocean system to the annual variation in the solar radiation. As shown in Figs. 3 and 4, the global monsoon dominates the seasonal variation of the tropical precipitation and the lower tropospheric circulation. It is important to distinguish the monsoon regime from other regimes in the globe, because the global monsoon defines essential features of the Earth's climate, and their rain affects over two-thirds of the world's population.

4.1. Monsoon precipitation index (MPI)

A contrast between the rainy summer and the dry winter and the accompanied reversal of wind direction between the summer and winter are two dominant characteristics of the monsoon climate (Trenberth et al., 2000; Webster, 2006). While surface winds have been traditionally used to define monsoon (Ramage, 1971), precipitation is considered here as an alternative fundamental variable for defining the monsoon climate because the latent heat released in monsoon precipitation drives the annual variations of the tropical circulation and because the monsoon rainfall is the key parameter in global hydrological cycle that is most influential on human being and society.

In the previous section, we have demonstrated that the global monsoon is primarily described by the first two major modes of the annual variation and these two modes can be well represented by the contrasts between solstitial seasons (JJAS versus DJFM) and between the transitional seasons (AM versus ON). These findings allow us to depict the structure of the global monsoon in terms of the combination of the first two modes. As shown in Fig. 5, summation of the normalized PC1 and PC2 weighted by their percentage variances, namely PC1 × 71% + PC2 × 13%, results in a combined PC, which has a zero value around April and October. Therefore, the boreal summer (austral winter) monsoon season may be considered consisting of May, June, July, August, and September, or MJJAS, while the boreal winter (austral summer) consists of November, December, January, February, and March, or NDJFM. The annual range can be defined by the local summer-minus-winter precipitation, i.e., MJJAS precipitation minus NDJFM precipitation in the NH and NDJFM minus MJJAS in the SH.

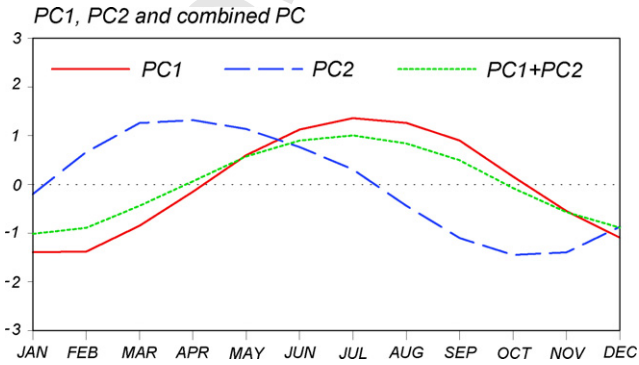

Fig. 5. Normalized PC1, PC2 of the multi-variable EOF modes and the sum of PC1 and PC2 weighted by their percentage variance, namely, PC1 × 71% + PC2 × 13%.

Please cite this article in press as: Wang, B., Ding, Q., Global monsoon: Dominant mode of annual variation in the tropics, Dyn. Atmos. Oceans (2008), doi:10.1016/j.dynatmoce.2007.05.002

To objectively delineate the monsoon's domain in the global tropics, we proposed a simple MPI, which is defined by the ratio of the annual range over the annual mean precipitation, i.e.,

$$\text{MPI} = \frac{\text{Annual range of precipitation}}{\text{Annual mean precipitation}}$$

The annual range measures the rainfall contrast between wet summer and dry winter. The MPI measures the relative amplitude of the annual variation with respect to its annual mean. Therefore, MPI reflects collective information regarding the summer–winter contrast and the relative intensity of the local summer rainfall compared with the annual mean precipitation. A typical monsoon climate is characterized by a significant annual range (the wet summer and dry winter contrast) and a concentration of rainfall during the local summer. As such, the larger the MPI, the more the precipitation characteristics are typical and are qualified as a monsoon climate.

4.2. Global monsoon precipitation domain

Fig. 6a presents the spatial distribution of the MPI. Note that the negative value of MPI (the brown color area in Fig. 6a) implies a Mediterranean regime, which features a wet winter and a dry summer. In Fig. 6a, we determine the monsoon precipitation domain as the regions in which MPI greater than 0.5 and the annual range greater than 300 mm. The first criterion distinguishes the monsoon climate from the equatorial perennial rainfall regime where the annual range is

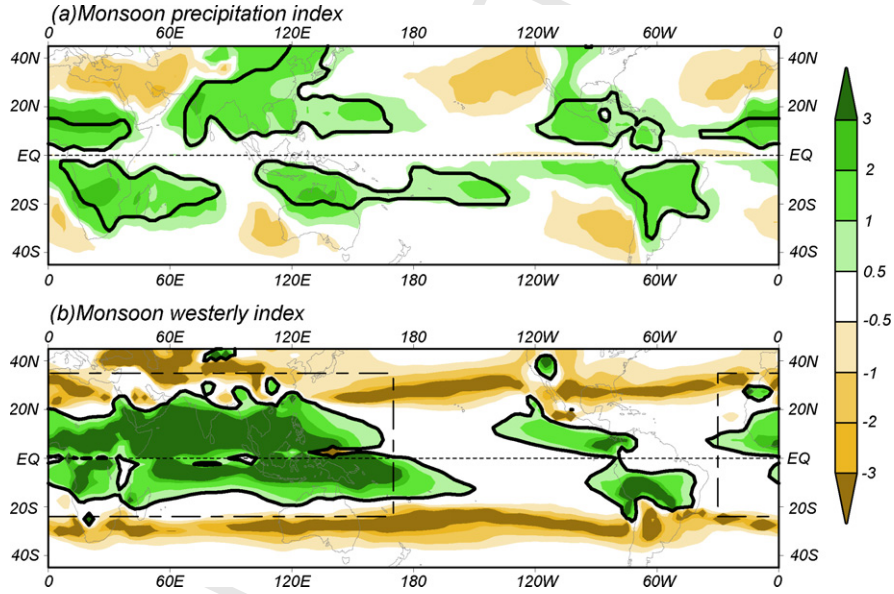

Fig. 6. (a) Monsoon precipitation index, MPI (color shading) and the monsoon precipitation domain outlined by the black curves. The definition of MPI is referred to the text. The monsoon precipitation domain here is defined by MPI > 0.5 and the annual range of precipitation is greater than 300 mm. The data used are CMAP precipitation measurements. (b) Monsoon westerly index, MWI (color shading) and the monsoon westerly domain outlined by the black curves. The definition of MWI is referred to the text. The monsoon westerly domain here is defined by MWI > 0.5. The wind data used are 850 hPa zonal wind component derived from NCEP2. The dashed rectangle indicates the monsoon domain defined by Ramage (1971).

Please cite this article in press as: Wang, B., Ding, Q., Global monsoon: Dominant mode of annual variation in the tropics, Dyn. Atmos. Oceans (2008), doi:10.1016/j.dynatmoce.2007.05.002

relatively small compared to its annual mean. The second criterion distinguishes monsoon from subtropical arid and semi-arid regimes.

The major monsoon rainy regions that are defined by MPI > 0.5 and the annual range > 300 mm identified in Fig. 6a include Southeast Asia, Indonesia–Australia, North and South Africa, and North and South America. Some oceanic regions are also found to typify monsoon rainfall patterns: the Philippine Sea, the Southwest Indian Ocean, and the subtropical mid-South Pacific. In general, the monsoon regions tend to reside on each side of the equatorial perennial rainfall regions (Fig. 1a).

The Asian monsoon regions defined here are in good agreement with the monsoon domains that have been previously defined based upon more complex multiple criteria (Wang and Lin, 2002). Globally, the monsoon domains defined here are in good agreement with those defined by Wang and Ding (2006), who used JJA and DJF defining annual range along with the following two criteria: (a) an annual range greater than 180 mm and (b) a local summer precipitation that exceeds 35% of the annual total precipitation. These comparisons lend confidence to this simple index with the two threshold values.

Of note is that the determination of the first threshold value (0.5) is empirical. Sensitivity tests have been carried out to examine how the global monsoon domain varies with choices of the threshold value of MPI (Fig. 7). The size of the domain decreases as MPI increases from 0 to 1. When MPI = 0, the continental monsoon regions remain the same as MPI = 0.5, but the oceanic monsoon regions expand and include most part of the ITCZ, SPCZ, and Southwest Indian Ocean Convergence Zone. On the other hand, when MPI = 1, the oceanic monsoon regions tend to disappear and the domains of the East Asian and Venezuelan monsoons are remarkably reduced. However, when MPI is in the range of 0.4–0.6, the resultant global monsoon domain is not sensitive to the threshold value of MPI. The sensitivity tests suggest that the threshold value of 0.5 is an adequate choice.

It is interesting to point out that the global monsoon domain occupies about 19.4% of the total area of Earth's surface, but the monsoon rainfall accounts for 30.8% of the total precipitation on globe. This implies that the monsoon regions represent the most concentrated rainfall regions in the world. In the non-monsoon tropical regions between 30°S and 30°N, for instance, the fractional area is 33.7% while the fractional precipitation is 37.5%. In the extratropical non-monsoon regions beyond 30°S and 30°N, the fractional area is 46.8%, while the fractional precipitation is 31.7%. These statistics were made based on CMAP data. There are significant differences between the GPCP data and CMAP data, suggesting considerable uncertainties in the estimated global precipitation. But the conclusion concerning the high concentration of rainfall in the monsoon regions remains valid.

4.3. Global monsoon westerly domain

The monsoon climate is also characterized by an annual reversal of the low-level winds. Using 850 hPa zonal winds, we can define a monsoon westerly index (MWI) in the same way that the MPI was defined, except using 850 hPa zonal winds to replace precipitation and no restriction is applied to the magnitude of annual range. Now, the numerator measures the annual range between the local summer westerly and the winter easterly components. Denominator measures the annual mean zonal wind speed. This westerly index is expected to depict tropical monsoon domain.

Fig. 6b shows the monsoon domain as depicted by MWI when its value is greater than 0.5. The tropical Asian–Australia–African monsoon regions are picked up by this index very well. It

Please cite this article in press as: Wang, B., Ding, Q., Global monsoon: Dominant mode of annual variation in the tropics, Dyn. Atmos. Oceans (2008), doi:10.1016/j.dynatmoce.2007.05.002

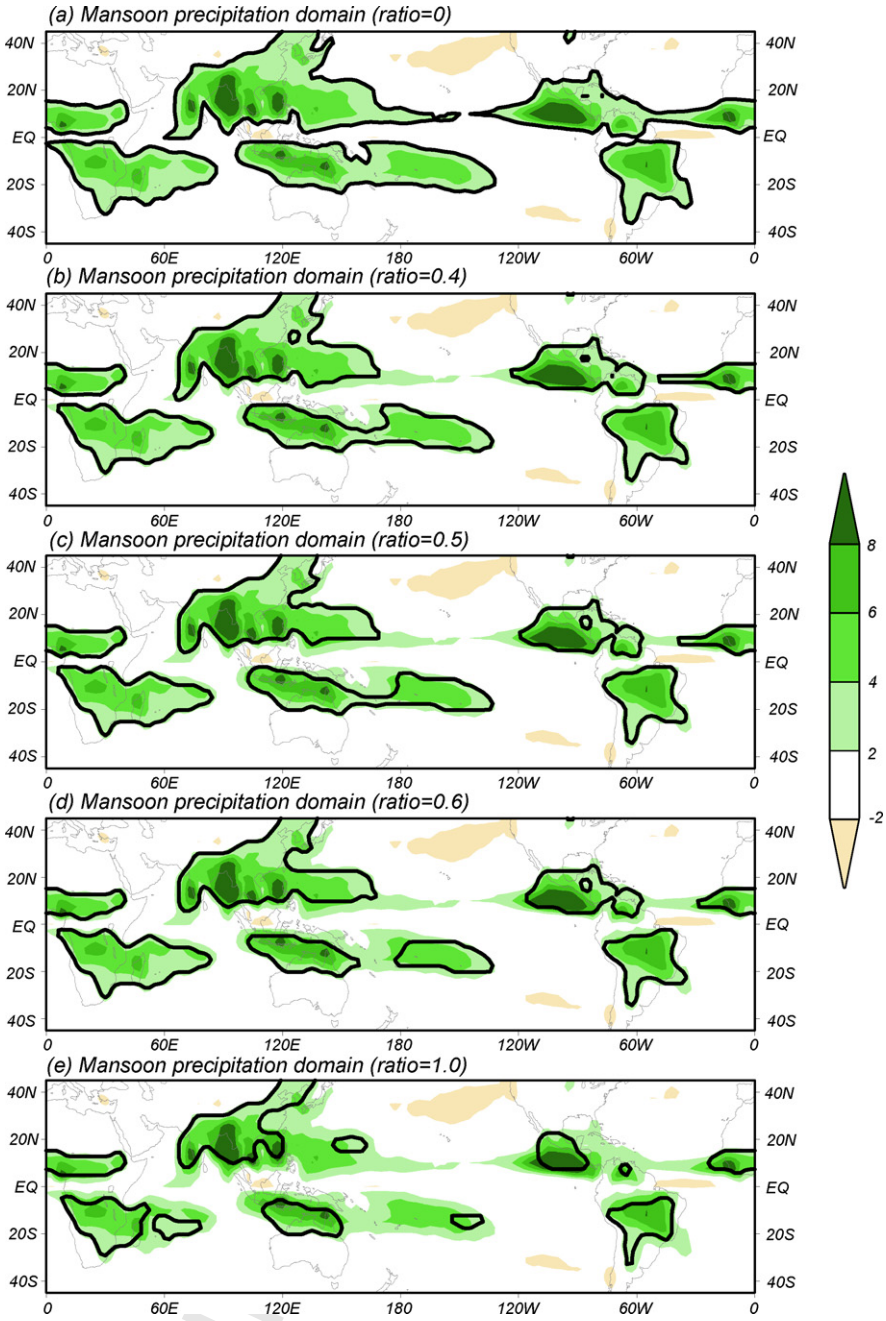

Fig. 7. Monsoon precipitation domains (black curves) defined by monsoon precipitation index (MPI) greater than (a) 0, (b) 0.4, (c) 0.5, (d) 0.6, and (e) 1.0, respectively, and the annual range (shading, unit: mm day^{-1}) greater than 300 mm.

Please cite this article in press as: Wang, B., Ding, Q., Global monsoon: Dominant mode of annual variation in the tropics, Dyn. Atmos. Oceans (2008), doi:10.1016/j.dynatmoce.2007.05.002

is in an excellent agreement with previous definitions made by Ramage (1971) and others using much more complex criteria. The American monsoons are weak in terms of annual reversal of zonal winds but still discernible. It is important to point out that the monsoon westerly domain and monsoon precipitation domain are physically consistent when one recognizes that precipitation functions as a latent heat source that drives the wind change. The westerly domains are situated to the equatorward and westward sides of the precipitation domains as expected from a Rossby wave response to the precipitation heat sources.

Note that beyond the tropics, the low-level winds also reverse annually (the brown shaded regions), but they are not monsoons because the annual wind reversal is in the opposite direction to that of the tropical monsoon. These mid-latitude reversals of wind arise from an annual variation of the mid-latitude westerlies: the westerlies shift poleward during local summer and equatorward during local winter, which results in a decreased westerly during the local summer and a decreased easterly during the local winter. Accordingly, in those regions, wet winters and dry summers prevail, reflecting a climate typical of the Mediterranean, not the monsoon regime. The annual reversal of winds in the mid-North Pacific and mid-North Atlantic should not be mistaken as a monsoon climate regime.

5. The annual cycles in three reanalysis datasets

Global reanalysis data produced independently by major operational centers, such as the National Centers for Environmental Prediction (NCEP), the European Centre for Medium-Range Weather Forecasts (ECMWF) and Japan Meteorological Agency (JMA) have been widely used to examine the global hydrological cycle and to understand its associated atmospheric circulation (e.g., Trenberth and Guillemot, 1998; Roads et al., 2002). These reanalyses are produced by assimilating the models' first guess fields to various observed variables such as pressure, temperature, wind, and humidity. However, precipitation fields are derived products, which depend strongly on the model physics and parameterization schemes. Thus, the precipitation in a reanalysis is model-dependent and not directly constrained by observations. We anticipate uncertainties in the precipitation and hydrological cycle in the reanalysis datasets, due to insufficient and inaccurate observations used for the reanalyses as well as deficiencies within the assimilation system. One of the purposes of the present study is to assess objectively the uncertainties in these reanalyses by using well designed metrics.

In this section, we apply the three-parameter metrics and the global monsoon domain proposed in the previous section to assess the performances of three reanalysis datasets, the NCEP2, ERA40, and JRA25. For an objective assessment, we used a pattern correlation coefficient (PCC) and a root mean square error (RMSE). The former represents the domain-averaged correlation coefficients between the reanalysis (prediction) and the actual observation at each grid point. The latter measures the domain-averaged RMSE of the reanalysis and its prediction compared to actual observation within each grid.

Fig. 8 compares the spatial patterns of the annual mean, solstitial, and equinoctial asymmetric modes derived from the observed CMAP and those derived from the NCEP2, ERA40, and JRA25 reanalysis datasets. To quantify observational uncertainty, we first computed the PCC between the two observed datasets, i.e., the CMAP and the Global Precipitation Climatology Project (GPCP, Adler et al., 2003) rainfall. The PCCs between the CMAP and GPCP are all 0.96 for the annual mean, and the first and second annual variation mode. The domain-averaged RMSE are 0.73, 0.94 and 0.55 mm/day, respectively, for the annual mean, and the first and second mode of annual variations between the CMAP and GPCP datasets.

Please cite this article in press as: Wang, B., Ding, Q., Global monsoon: Dominant mode of annual variation in the tropics, Dyn. Atmos. Oceans (2008), doi:10.1016/j.dynatmoce.2007.05.002

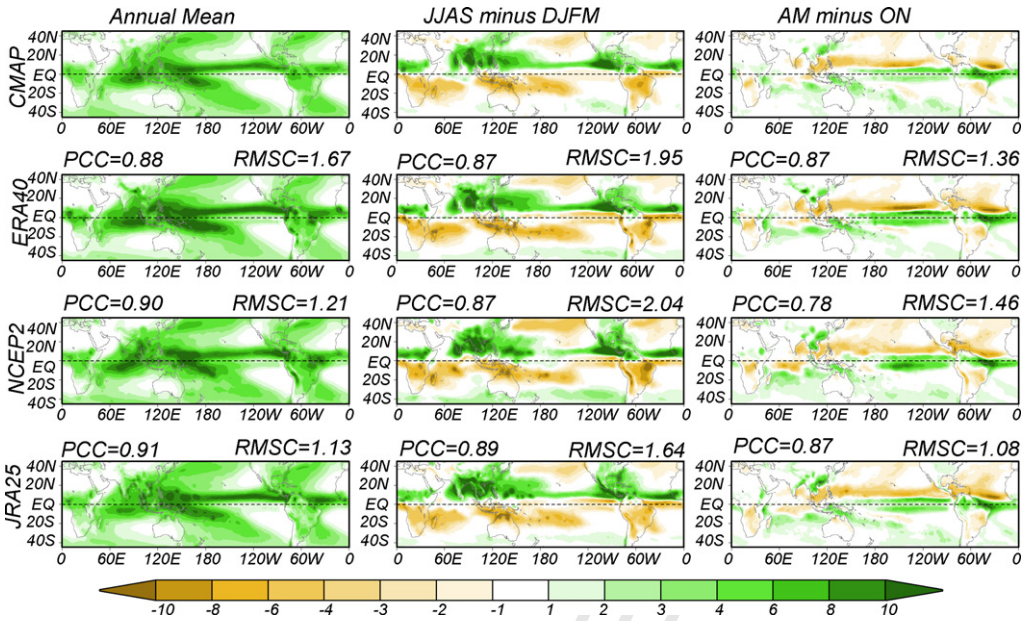

Fig. 8. [Left to right] Annual mean precipitation, the solstitial mode (JJAS minus DJFM precipitation), and the equinoctial asymmetric mode (AM minus ON precipitation) that are derived, respectively, from CMAP data, the ERA40, NCEP2, and JRA25 reanalysis (from top to bottom). The PCC indicates pattern correlation coefficients with the CMAP and the RMSE indicates root mean square error with reference to observed CMAP between 45°S and 45°N.

Given this uncertainty of satellite observation in mind, the annual mean field was considered to be well captured by JRA25 (PPC: 0.91 and RMSE: 1.13), NCEP2 (PCC: 0.90 and RSME; 1.21) and ERA40 (PCC: 0.88 and RMSE: 1.67). The JRA25 is the best and ERA40 the worst among the three. Concerning the annual variations, the three reanalysis datasets have comparable PCC and RMSE on the first EOF, but the ERA40 and JRA25 reproduces better equinoctial asymmetry mode compared to the NCEP2. Overall, JRA25 is consistently better than the other two reanalysis datasets.

Another desirable attribute is to examine the capability of the reanalyses in capturing the global monsoon precipitation domain (Fig. 6a). The global monsoon domains in the three reanalysis datasets are shown in Fig. 9 in comparison with observed domain derived by using CMAP. In general, the monsoon domains in the three reanalysis datasets resemble the observed, especially the Asian and South African continental monsoon, Indonesian and Australian monsoon, and the North African and South American monsoons. However, the oceanic monsoon regions in the tropical western North Pacific and South Pacific, as well as the North American and Venezuelan monsoons are less well delineated. In addition, the NCEP2 overestimates the annual range over the South Indian Ocean. Overall, the JRA25 and ERA40 reanalysis data reproduce the more realistic features of the observed global monsoon precipitation domain. Further comparison of the annual ranges in the observed global monsoon domain indicates that JRA25 has the best performance (Table 1).

The three reanalyses have a common weakness, that is, they do not capture the monsoon regime faithfully in the North American and East Asian sectors. The models tend to enlarge the precipitation domain in USA and Caribbean Sea while reduce the domain in Venezuela. In

Please cite this article in press as: Wang, B., Ding, Q., Global monsoon: Dominant mode of annual variation in the tropics, Dyn. Atmos. Oceans (2008), doi:10.1016/j.dynatmoce.2007.05.002

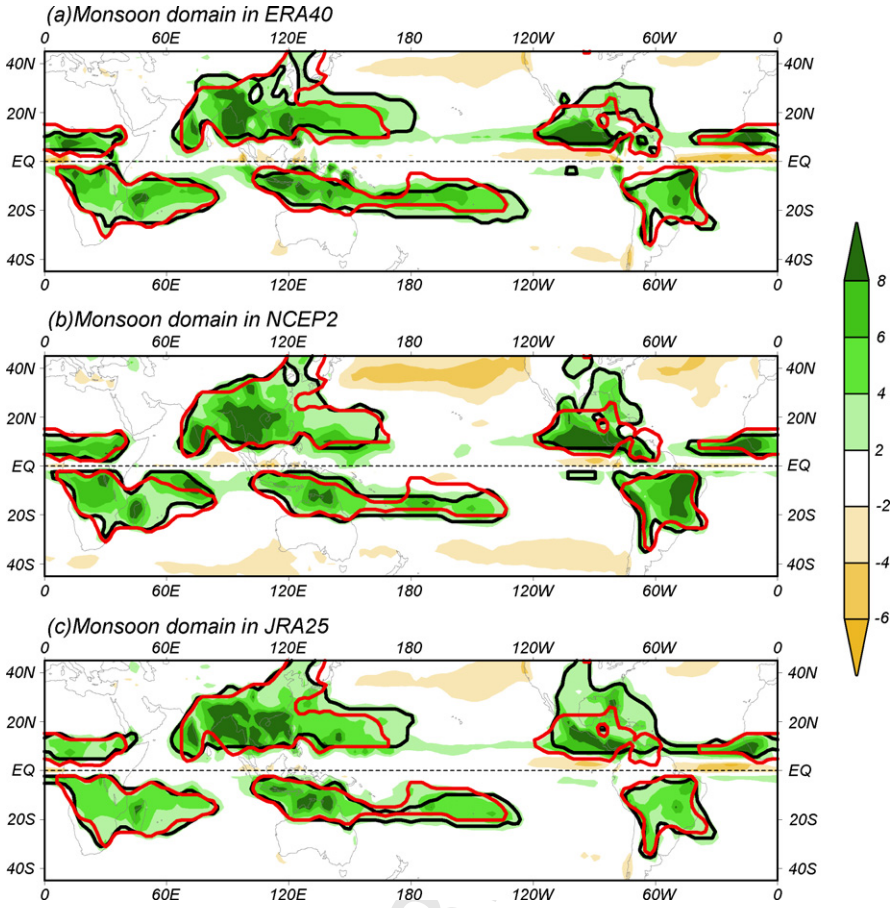

Fig. 9. Global monsoon domains captured in the (a) ERA40, (b) NCEP2, and (c) JRA25 reanalysis datasets (black curves). Red curves indicate the observed global monsoon domain captured in the CMAP data. The shadings in each panel represent annual range of precipitation (in unit of mm day^{-1}).

addition, the ERA40 and NCEP2 have problems with delineation of the East Asian monsoon domain but JRA25 is obviously better in the same region. The East Asia and North America are regions where the east–west land–ocean thermal contrast and meridional hemispheric thermal contrast coexist. The models have difficulty to capture the correct annual march of the circulation

Table 1
Pattern correlation coefficients (PCC) and root mean square errors (RMSE) of the annual range in three reanalysis datasets and ensemble mean within observed global monsoon domain with reference to observation (CMAP)

	PCC	RMSE
ERA40	0.91	2.32
NCEP2	0.91	2.47
JRA25	0.92	2.08
Ensemble	0.94	1.78

The annual range is defined by the local summer-minus-winter precipitation, i.e., MJJAS precipitation minus NDJFM precipitation in the NH and NDJFM minus MJJAS in the SH.

Please cite this article in press as: Wang, B., Ding, Q., Global monsoon: Dominant mode of annual variation in the tropics, Dyn. Atmos. Oceans (2008), doi:10.1016/j.dynatmoce.2007.05.002

Table 2
Pattern correlation coefficients (PCC) and root mean square errors (RMSE) of the annual mean, JJAS minus DJFM and AM minus ON modes in three reanalysis datasets and ensemble mean between 45°S and 45°N with reference to observation (CMAP)

	Annual mean		JJAS minus DJFM		AM minus ON	
	PCC	RMSE	PCC	RMSE	PCC	RMSE
ERA40	0.88	1.67	0.87	1.95	0.87	1.36
NCEP2	0.90	1.21	0.87	2.04	0.78	1.46
JRA25	0.91	1.13	0.89	1.64	0.87	1.08
Ensemble	0.93	1.12	0.91	1.53	0.88	1.07

systems, such as the western North Pacific Subtropical High and the North Atlantic Subtropical High during boreal summer, which are critical systems for reproducing the monsoon precipitation.

Of interest is that the ensemble mean of the three analysis datasets, which is obtained by a simple arithmetic average, is considerably superior to any of the individual reanalysis data in representing annual mean, major modes of annual cycle, and the global monsoon domain. The comparison of the ensemble mean with individual models' performance is presented in Table 2. It is recommended that the ensemble mean of three reanalysis datasets be used for better representation of the precipitation climatology and for improved global water cycle budget.

6. Conclusion

In this paper, we described the spatial structures of the time-mean and seasonal variation of the tropical precipitation and low-level circulations in response to solar radiative forcing and evaluated how well the three reanalysis datasets (ERA40, NCEP2, and JRA25) represent the annual cycle of the tropical precipitation. The major findings are summarized as follows:

- The climatology of the tropical precipitation and low-level circulation can be well depicted by a three-parameter metrics: the annual mean, a solstitial mode, and an equinoctial (spring-fall) asymmetric mode.
- The solstitial mode can be simply depicted by the June–September mean minus the December–March mean. The equinoctial asymmetric mode can be approximately depicted by the difference between the April–May mean and the October–November mean. Both modes depict annual cycle and together they account for 84% of the annual variance.
- The global monsoon precipitation domain can be delineated by a simple MPI, which is the local annual range of precipitation (MJJAS minus NDJFM in the NH and NDJFM minus MJJAS in the SH) normalized by the annual mean precipitation. The monsoon domain can be defined by annual range exceeding 300 mm and the MPI exceeding 50%.
- We propose that a region that exhibits both strong annual reversal in lower tropospheric winds and a "wet summer–dry winter" contrast may be regarded as a "strong" monsoon region. On the other hand, the American monsoons and the oceanic monsoons in the subtropical Southwest Indian Ocean and mid-South Pacific may be considered as weak monsoons for which the wet summer–dry winter contrast is prominent but the annual reversal of winds is weak or absent.
- While the annual mean tropical boundary-layer circulation shows considerable hemispheric asymmetry, the upper level circulation shows a prominent symmetric pattern with respect to the equator. The latter results from the gross symmetry in the tropical precipitation heating.

Please cite this article in press as: Wang, B., Ding, Q., Global monsoon: Dominant mode of annual variation in the tropics, Dyn. Atmos. Oceans (2008), doi:10.1016/j.dynatmoce.2007.05.002

- All three reanalysis data (ERA40, NCEP2, and JRA25) capture precipitation climatology realistically. The JRA25 is better than the other two reanalysis datasets. The ensemble mean of the three analysis datasets, which is obtained by an arithmetic average, is superior to any of the individual reanalysis data in representing annual mean, major modes of annual cycle, and the global monsoon domain (Table 2).
- A common problem with the three reanalysis datasets is a failure to capture the monsoon regime realistically in the Southeast Asia-Philippine Sea and southeast North America-Caribbean Sea where the east–west land–ocean thermal contrast and meridional hemispheric thermal contrast coexist.

We recommend that ensemble mean of three reanalysis datasets be used for better representation of the global precipitation climatology and water vapor budget. We speculate that in the observation-void western North Pacific and North Atlantic Ocean, the reanalyses heavily rely on model simulation, yet the present numerical models have difficulty in realistic simulation of the subtropical high system (Kang et al., 2002). Another conceivable reason is that the weather forecast models may under-represent tropical storm activities in both the western Pacific and North Atlantic Oceans due their inadequate resolution, which may affect climatological mean state in the reanalyses. The third possible reason is that in the current reanalysis the atmosphere is treated as a passive response to specified SST. However, the monsoon–ocean interaction is so active that neglect of the atmosphere–ocean interaction makes model simulation yield a wrong local SST–rainfall relationship over the WNP; and thus, treating atmosphere as a slave may be inherently unable to simulate summer monsoon rainfall variations in the heavily precipitating regions (Wang et al., 2004). It is recommended that future reanalysis should be carried out with coupled atmosphere and ocean models (Wang et al., submitted for publication). The precise cause calls for further study.

Acknowledgements

This study is supported by the Climate Dynamics Program of National Science Foundation, the NOAA OGP through CLIVAR/Pacific Program, and by APEC Climate Center. The International Pacific Research Center is in part sponsored by Japan Agency for Marine-Earth Science and Technology. SOEST number xxxx and IPRC number yyy.

References

Adler, R.F., et al., 2003. The Version 2 Global Precipitation Climatology Project (GPCP) Monthly Precipitation Analysis (1979-Present). J. Hydrometeorol. 4, 1147–1167.

Chang, C.-P., Wang, Z., McBride, J., Liu, C.H., 2005. Annual cycle of Southeast Asia—Maritime Continent rainfall and the asymmetric monsoon transition. J. Climate 18, 287–301.

Charney, J., 1971. Tropical cyclogenesis and the formation of the intertropical convergence zone. Mathematical Problems of Geo-physical Fluid Dynamics. In: Reid, W.H. (Ed.), Lectures in Applied Mathematics, vol. 13. American Mathematical Society, pp. 355–368.

Gill, A.E., 1980. Some simple solutions for heat-induced tropical circulation. Q. J. R. Meteorol. Soc. 106, 447–462.

Guttman, N.B., 1989. Statistical descriptors of climate. Bull. Am. Meteorol. Soc. 70, 602–607.

Hastenrath, S., 1991. Climate Dynamics of the Tropics. Kluwer Academic Publishers, Dordrecht.

Kanamitsu, M., Ebisuzaki, W., Woollen, J., Yang, S.-K., Sling, J.J., Fiorino, M., Potter, G.L., 2002. NCEP-DOE AMIP-II Reanalysis (R-2). Bull. Am. Meteorol. Soc. 83, 1631–1643.

Kang, I.-S., et al., 2002. Intercomparison of the Climatological variations of Asian summer monsoon precipitation simulated by 10 GCMs. Climate Dyn. 19, 383–395.

Please cite this article in press as: Wang, B., Ding, Q., Global monsoon: Dominant mode of annual variation in the tropics, Dyn. Atmos. Oceans (2008), doi:10.1016/j.dynatmoce.2007.05.002

Lau, K.M., Chan, P.H., 1983. Short-term climate variability and atmospheric teleconnections from satellite-observed outgoing longwave radiation. Part II: lagged correlations. J. Atmos. Sci. 40, 2751–2767.

Matsuno, T., 1966. Quasi-geostrophic motions in the equatorial area. J. Meteorol. Soc. Jpn. 44, 25–43.

Meehl, G.A., 1987. The annual cycle and interannual variability in the tropical Pacific and Indian Ocean regions. Mon. Wea. Rev. 115, 27–50.

Mitchell, T.P., Wallace, J.M., 1992. On the annual cycle in equatorial convection and sea surface temperature. J. Climate 5, 1140–1152.

Onogi, K., et al. The JRA-25 Reanalysis. J. Meteorol. Soc. Jpn., submitted for publication. Q2

Philander, G., Gu, D., Halpern, D., Lambert, G., Lau, N.-C., Li, T., Pacanowski, R.C., 1996. Why the ITCZ is mostly north of the equator. J. Climate 9, 2958–2972.

Ramage, C.S., 1971. Monsoon Meteorology. Academic Press, New York.

Roads, J., Kanamitsu, M., Stewart, R., 2002. CSE Water and energy budgets in the NCEP-DOE reanalysis II. J. Hydrometeorol. 3, 227–248.

Trenberth, K.E., Guillemot, C.J., 1998. Evaluation of the atmospheric moisture and hydrological cycle in the NCEP/NCAR reanalyses. Climate Dyn. 14, 213–231.

Trenberth, K.E., Stepaniak, D.P., Caron, J.M., 2000. The Global monsoon as seen through the divergent atmospheric circulation. J. Climate 13, 3969–3993.

Uppala, S.M., et al., 2005. The ERA-40 re-analysis. Q. J. R. Meteorol. Soc. 131, 2961–3012.

Wang, B., 1992. The vertical structure and development of the ENSO anomaly mode during 1979–1989. J. Atmos. Sci. 49, 698–712.

Wang, B., 1994. Climatic regimes of tropical convection and rainfall. J. Climate 7, 1109–1118.

Wang, B., Li, T., 1994. Convective interaction with boundary-layer dynamics in the development of a tropical intraseasonal system. J. Atmos. Sci. 51, 1386–1400.

Wang, B., Lin, H., 2002. Rainy seasons of the Asian-Pacific monsoon. J. Climate 15, 386–398.

Wang, B., Kang, I.-S., Lee, J.-Y., 2004. Ensemble Simulations of Asian–Australian Monsoon Variability by 11 AGCMs. J. Climate 17, 803–818.

Wang, B., Ding, Q.-H., 2006. Changes in global monsoon precipitation over the past 56 years. Geophys. Res. Lett. 33, L06711, doi:10.1029/2005GL025347.

Wang, B., Lee, J.-Y., Kang, I.-S., Shukla, J., Kug, J.-S., Kumar, A., Schemm, J., Luo, J.-J., Yamagata, T., Park, C.-K. How accurately do coupled climate models predict the Asian–Australian monsoon interannual variability. Climate Dyn., submitted for publication.

Webster, P.J., 1972. Response of the tropical atmosphere to local steady forcing. Mon. Wea. Rev. 100, 518–541.

Webster, P.J., Magana, V.O., Palmer, T.N., Shukla, J., Tomas, R.A., Yanai, M., Yasunari, T., 1998. Monsoons: processes, predictability, and the prospects for prediction. J. Geophys. Res. 103, 14451–14510.

Webster, P.J., 2006. The coupled monsoon system. In: Wang, Bin (Ed.), The Asian Monsoon. Springer-Verlag.

Xie, P., Arkin, P.A., 1997. Global precipitation: a 17-year monthly analysis based on gauge observations, satellite estimates, and numerical model outputs. Bull. Am. Meteorol. Soc. 78, 2539–2558.

Please cite this article in press as: Wang, B., Ding, Q., Global monsoon: Dominant mode of annual variation in the tropics, Dyn. Atmos. Oceans (2008), doi:10.1016/j.dynatmoce.2007.05.002